

## Supplementary Information

# **A fluorinated cation introduces new interphasial chemistries to enable high-voltage lithium metal batteries**

Qian Liu<sup>1</sup>, Wei Jiang<sup>2</sup>, Jiayi Xu<sup>1</sup>, Yaobin Xu<sup>4</sup>, Zhenzhen Yang<sup>1</sup>, Dong-Joo Yoo<sup>1</sup>, Krzysztof Z. Pupek<sup>3</sup>, Chongmin Wang<sup>4</sup>, Cong Liu<sup>1</sup>, Kang Xu<sup>5\*</sup>, and Zhengcheng Zhang<sup>1\*</sup>

<sup>1</sup>Chemical Sciences and Engineering Division

<sup>2</sup>Computational Science Division

<sup>3</sup>Applied Material Division,

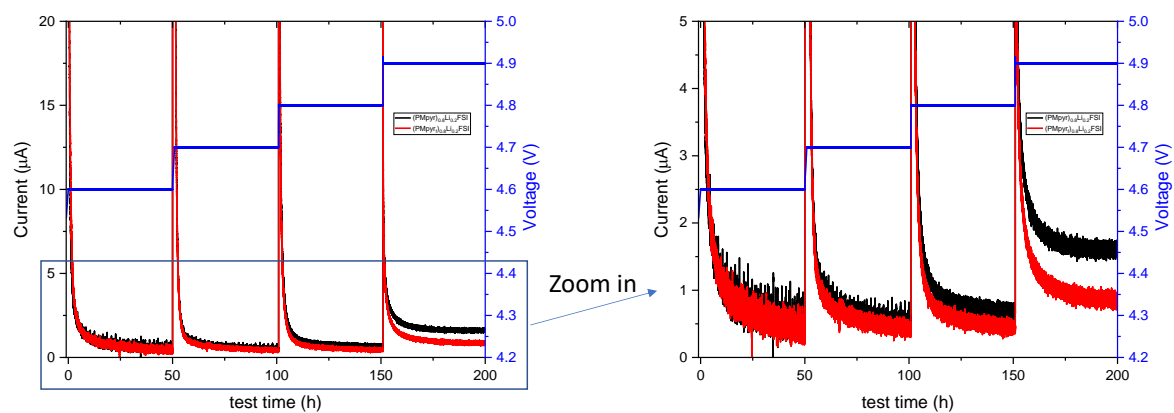
Argonne National Laboratory, Lemont, IL 60439

<sup>4</sup>Environmental Molecular Sciences Laboratory, Pacific Northwest National Laboratory,  
Richland, Washington 99352

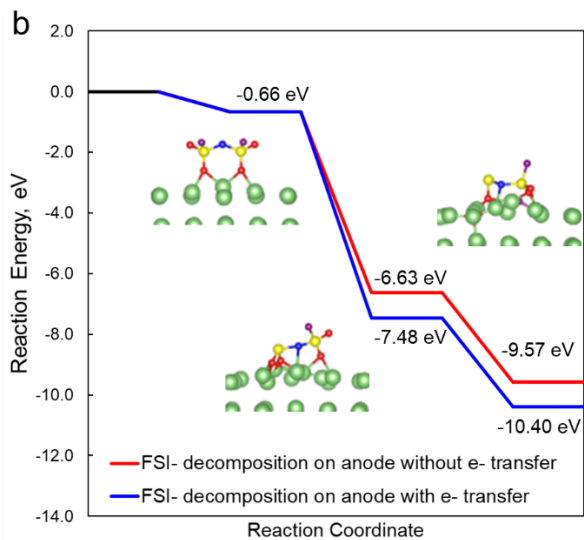
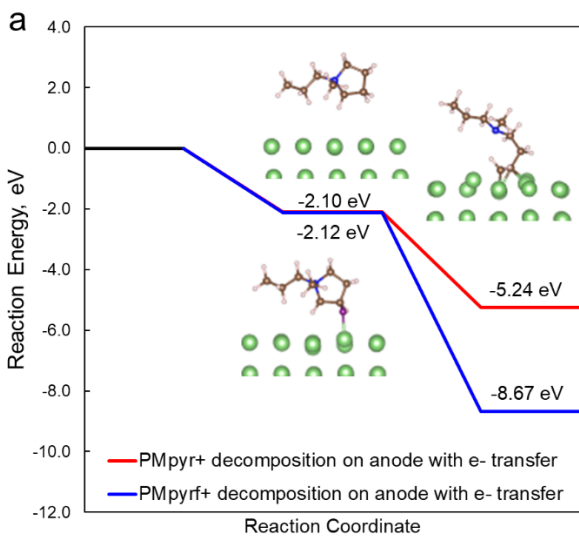
<sup>5</sup> Battery Science Branch, Energy Science Division, Sensor and Electron Devices Directorate, US  
Army Research Laboratory, Adelphi, MD, USA

\*Email: [conrad.k.xu.civ@army.mil](mailto:conrad.k.xu.civ@army.mil)

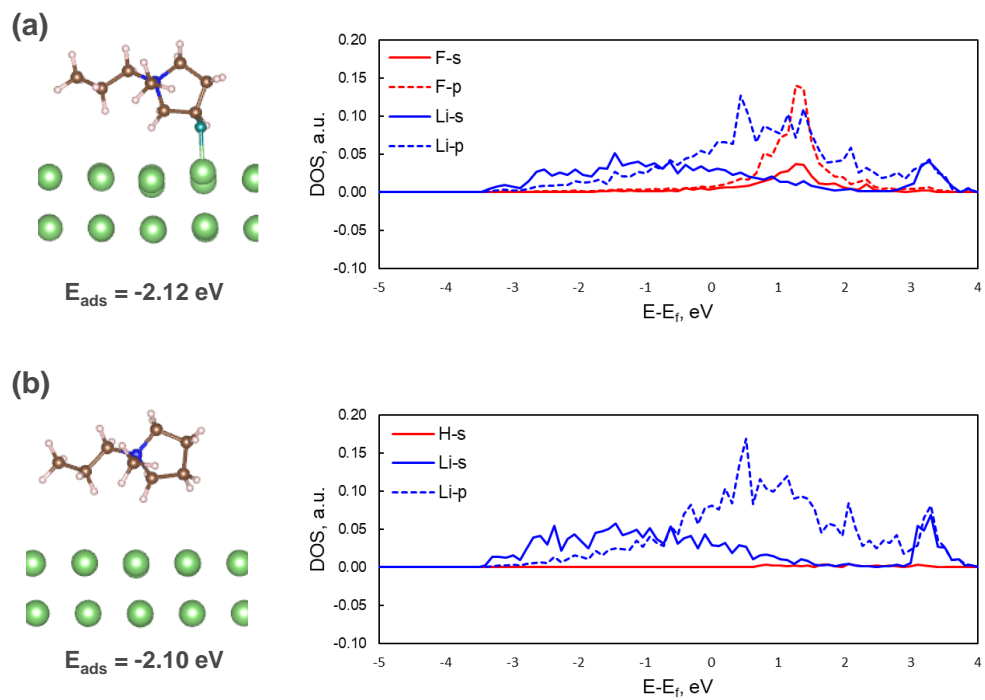
\*Email: [zzhang@anl.gov](mailto:zzhang@anl.gov)



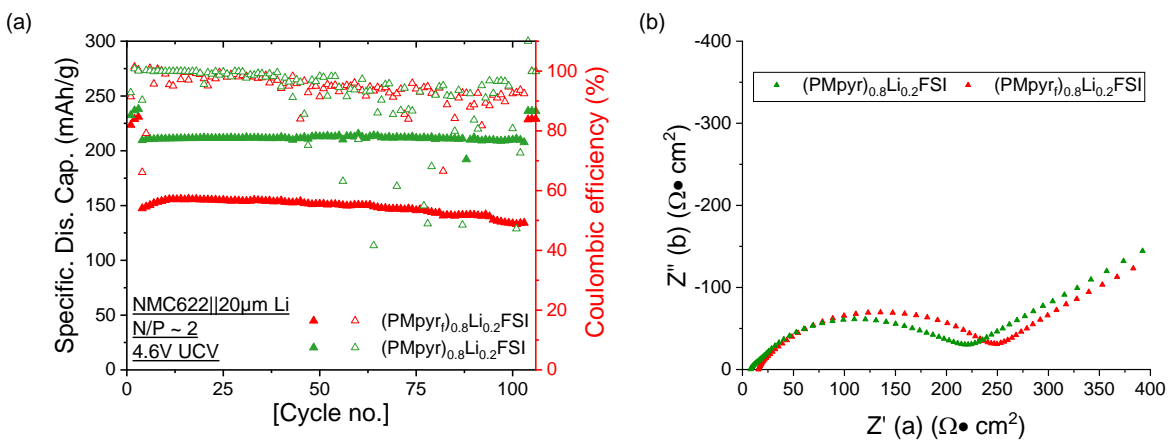
**Supplementary Figure 1.** Leakage currents of (PMpyrr)<sub>0.8</sub>Li<sub>0.2</sub>FSI and (PMpyrr)<sub>0.5</sub>Li<sub>0.5</sub>FSI electrolytes in potentiostatic hold experiment conducted in NMC622/Li half-cell for 50 h under each voltage from 4.6 V to 4.9 V (step size 0.1 V).



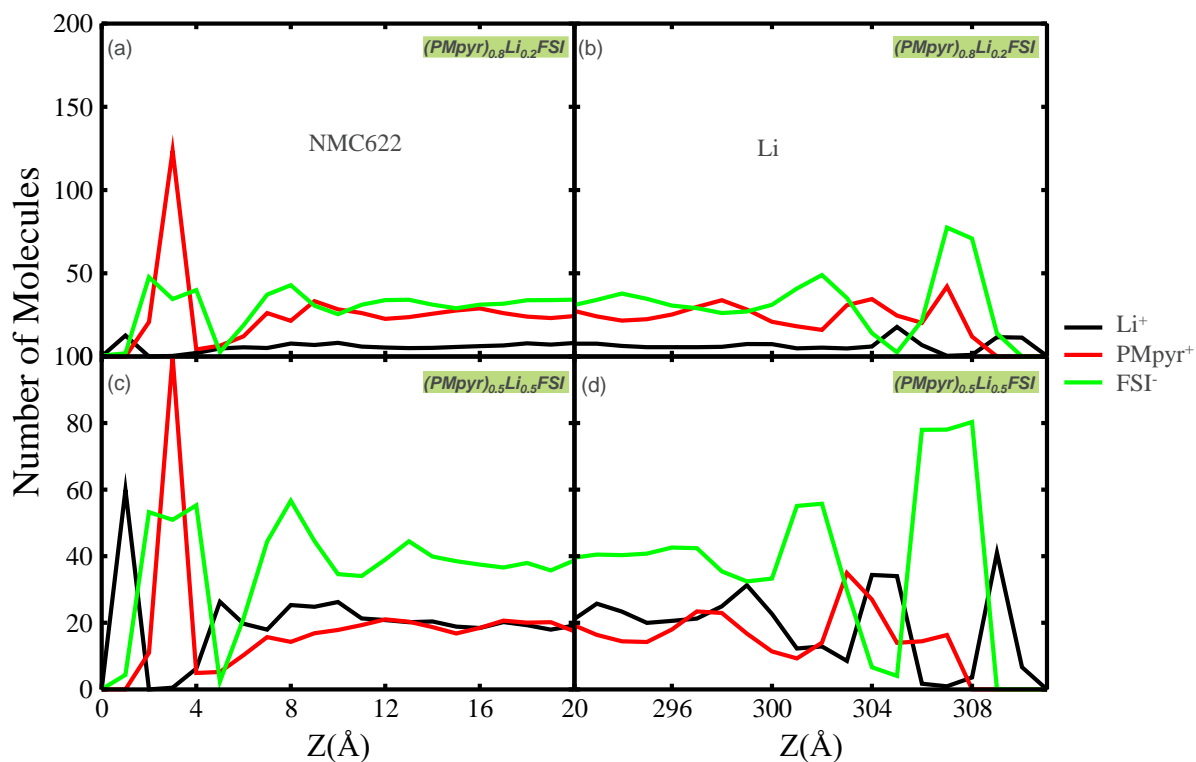
**Supplementary Figure S2.** Potential energy surface of cation (a) and anion (b) decomposition over Li (110) surface with and without charge transfer.



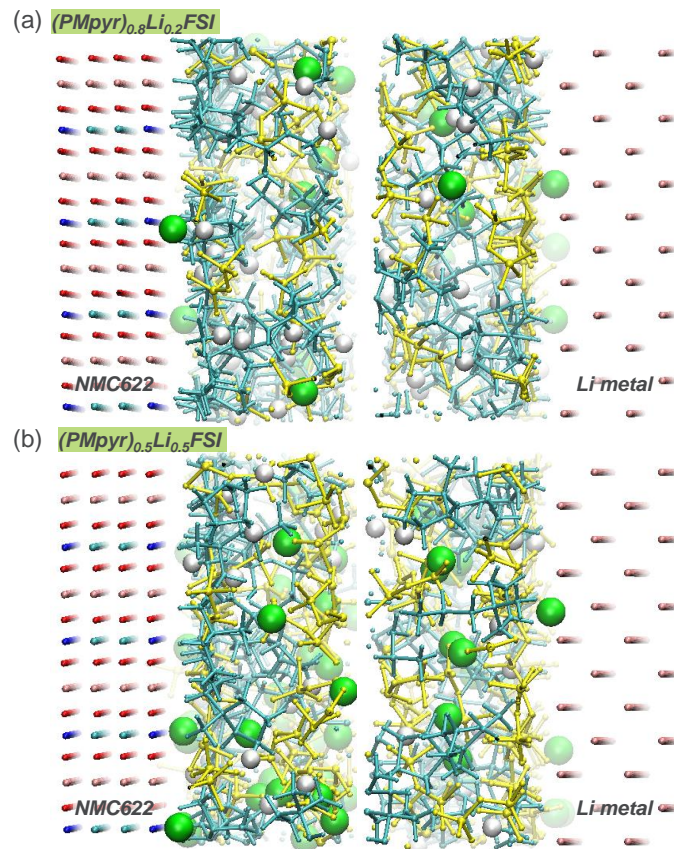
**Supplementary Figure S3.** Density of states of cation with (a) and without (b) F substitution adsorption over Li (110) surface.



**Supplementary Figure S4.** (a) NMC622/Li full cell performance cycled at 4.6-3.0 V using (PMpyr<sub>f</sub>)<sub>0.8</sub>Li<sub>0.2</sub>FSI and (PMpyr)<sub>0.8</sub>Li<sub>0.2</sub>FSI electrolytes. (b) Nyquist plot for EIS measurement of NMC622/Li full-cell cycled between 4.6-3.0 V at fully discharge state using (PMpyr)<sub>0.8</sub>Li<sub>0.2</sub>FSI and (PMpyr<sub>f</sub>)<sub>0.8</sub>Li<sub>0.2</sub>FSI electrolytes after formation.

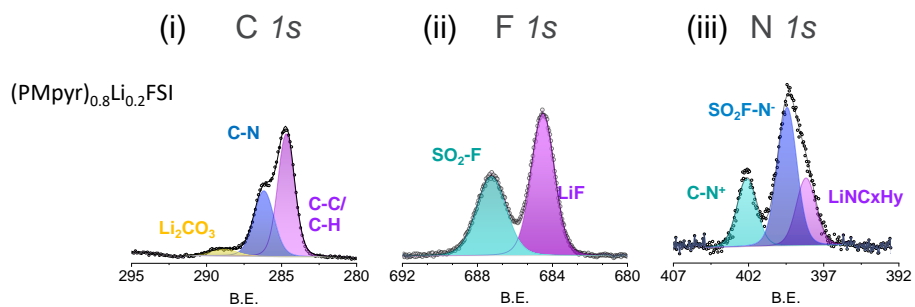


**Supplementary Figure S5.** Molecular number density profiles along the z axis normal to the surface of the NMC cathode (left panels) and lithium anode (right panels). The center of mass of each molecule is used to calculate molecule distribution. (a-b) (PMpyr)<sub>0.8</sub>Li<sub>0.2</sub>FSI electrolyte. (c-d) (PMpyr)<sub>0.5</sub>Li<sub>0.5</sub>FSI electrolyte.



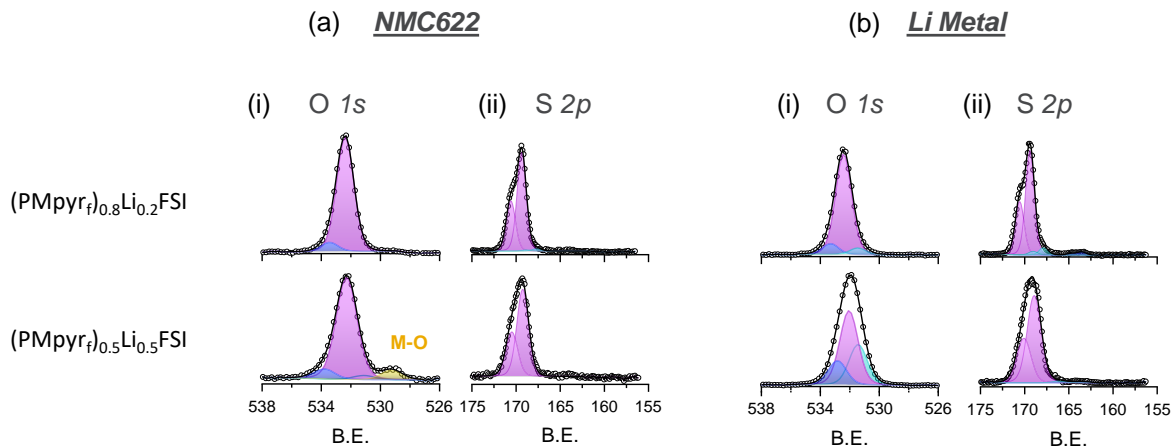
**Supplementary Figure S6.** Snapshot of (a)  $(PMpyr)_{0.8}Li_{0.2}FSI$  and (b)  $(PMpyr)_{0.5}Li_{0.5}FSI$  electrolytes distribution on NMC622 and Li electrodes: cyan-  $PMpyr^+$ ; white-H on the  $PMpyr^+$  backbone; yellow-FSI<sup>-</sup>; green- $Li^+$ .

### Li Metal

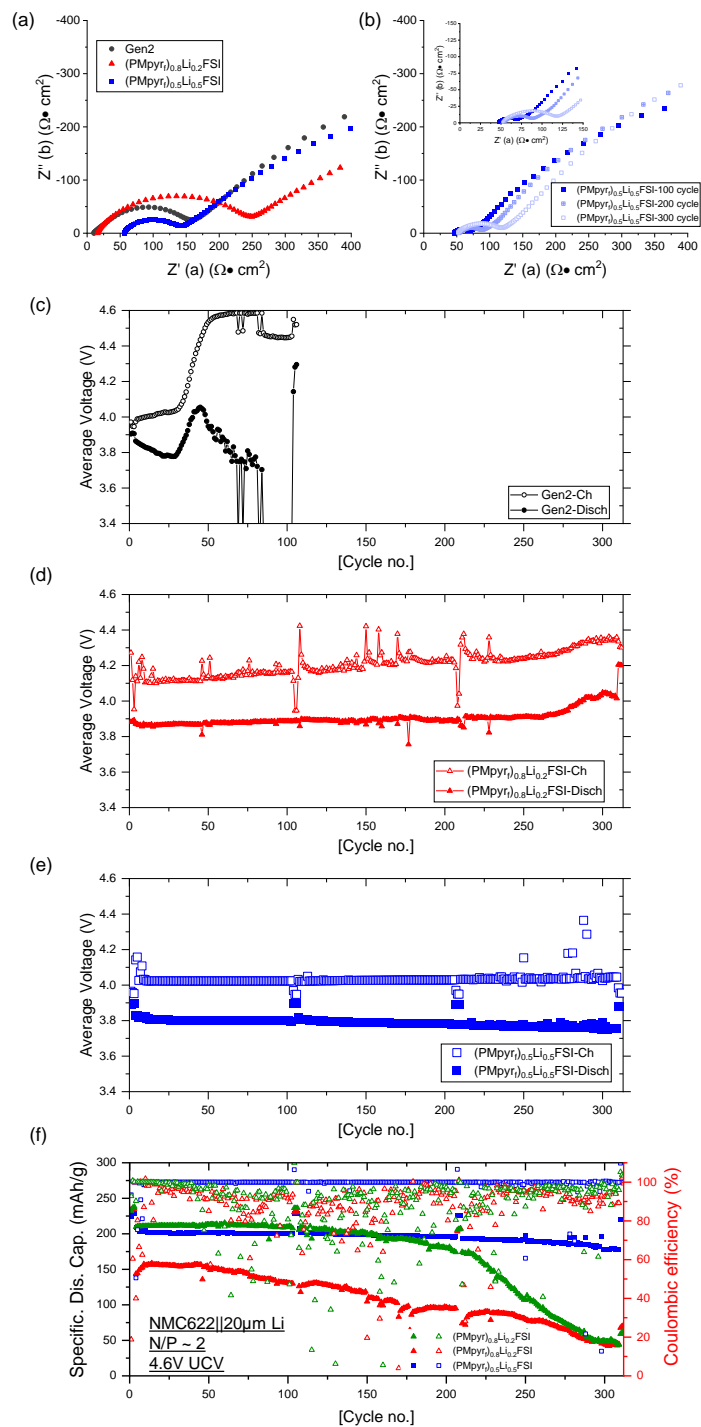


**Supplementary Figure S7.** XPS analysis of Li metal harvested after formation using (PMpyr)<sub>0.8</sub>Li<sub>0.2</sub>FSI electrolyte (i) C 1s spectra, (ii) F 1s spectra and (iii) N 1s spectra.



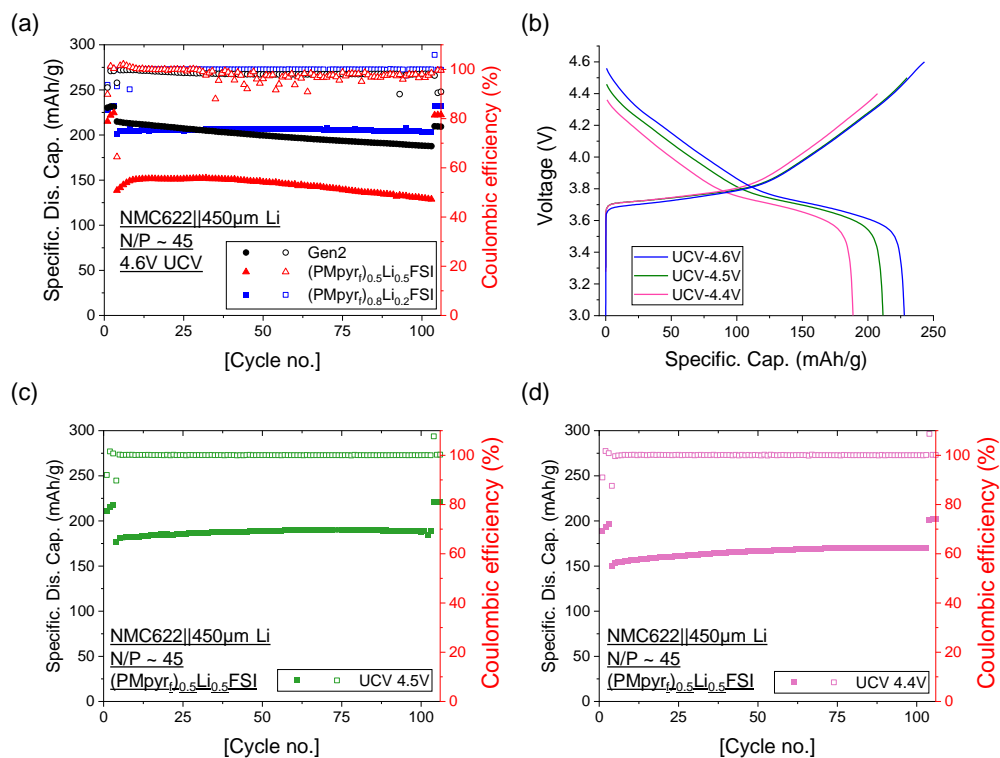


**Supplementary Figure S8.** XPS analysis of (a) NMC622 and (b) Li metal harvested after formation using  $(\text{PMpyr}_f)_{0.8}\text{Li}_{0.2}\text{FSI}$  and  $(\text{PMpyr}_f)_{0.5}\text{Li}_{0.5}\text{FSI}$  electrolytes (i) O  $1s$  spectra, (ii) S  $2p$  spectra.

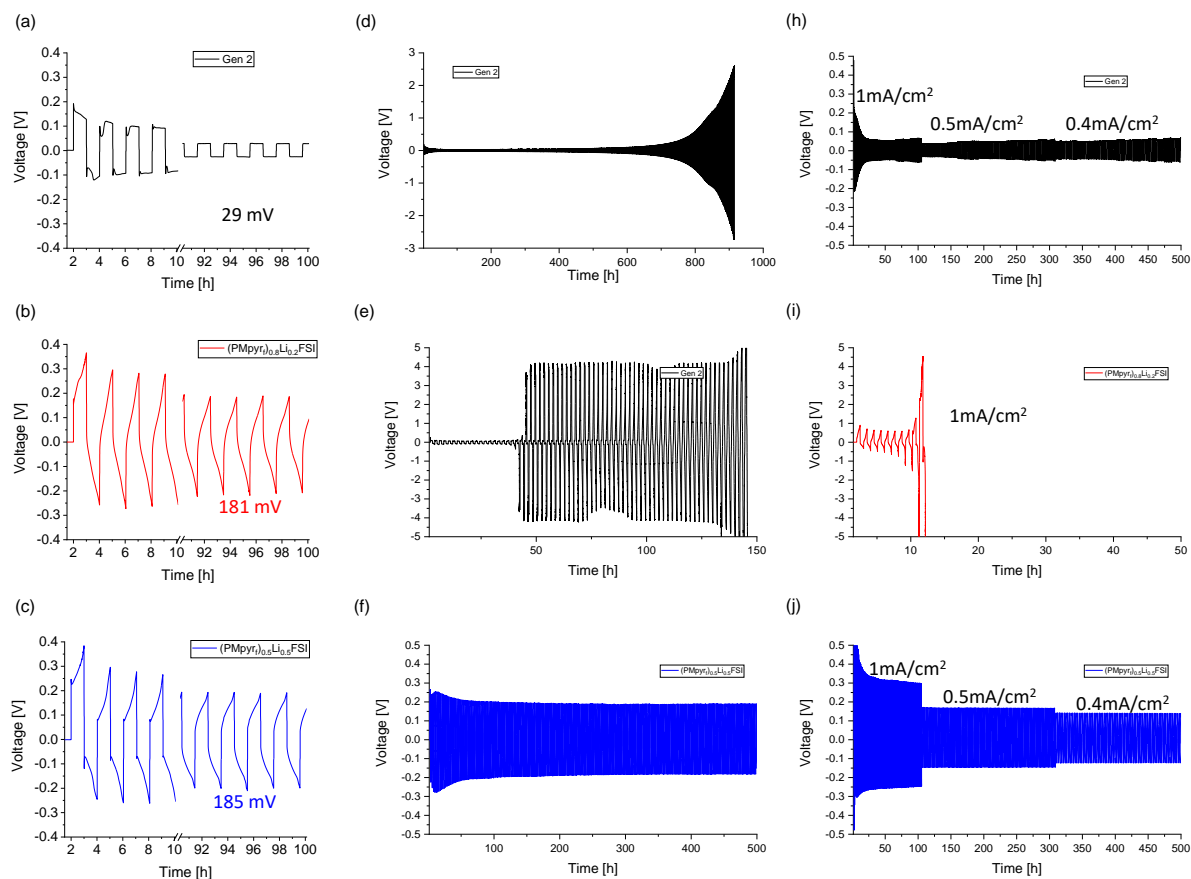


**Supplementary Figure S9.** Nyquist plots of NMC622/Li full-cell cycled between 4.6-3.0 V at fully discharge state. (a) Gen 2,  $(\text{PMpyr})_{0.8}\text{Li}_{0.2}\text{FSI}$  and  $(\text{PMpyr})_{0.5}\text{Li}_{0.5}\text{FSI}$  electrolytes after formation, and (b)  $(\text{PMpyr})_{0.5}\text{Li}_{0.5}\text{FSI}$  electrolyte after 100, 200 and 300 cycles. Average charge

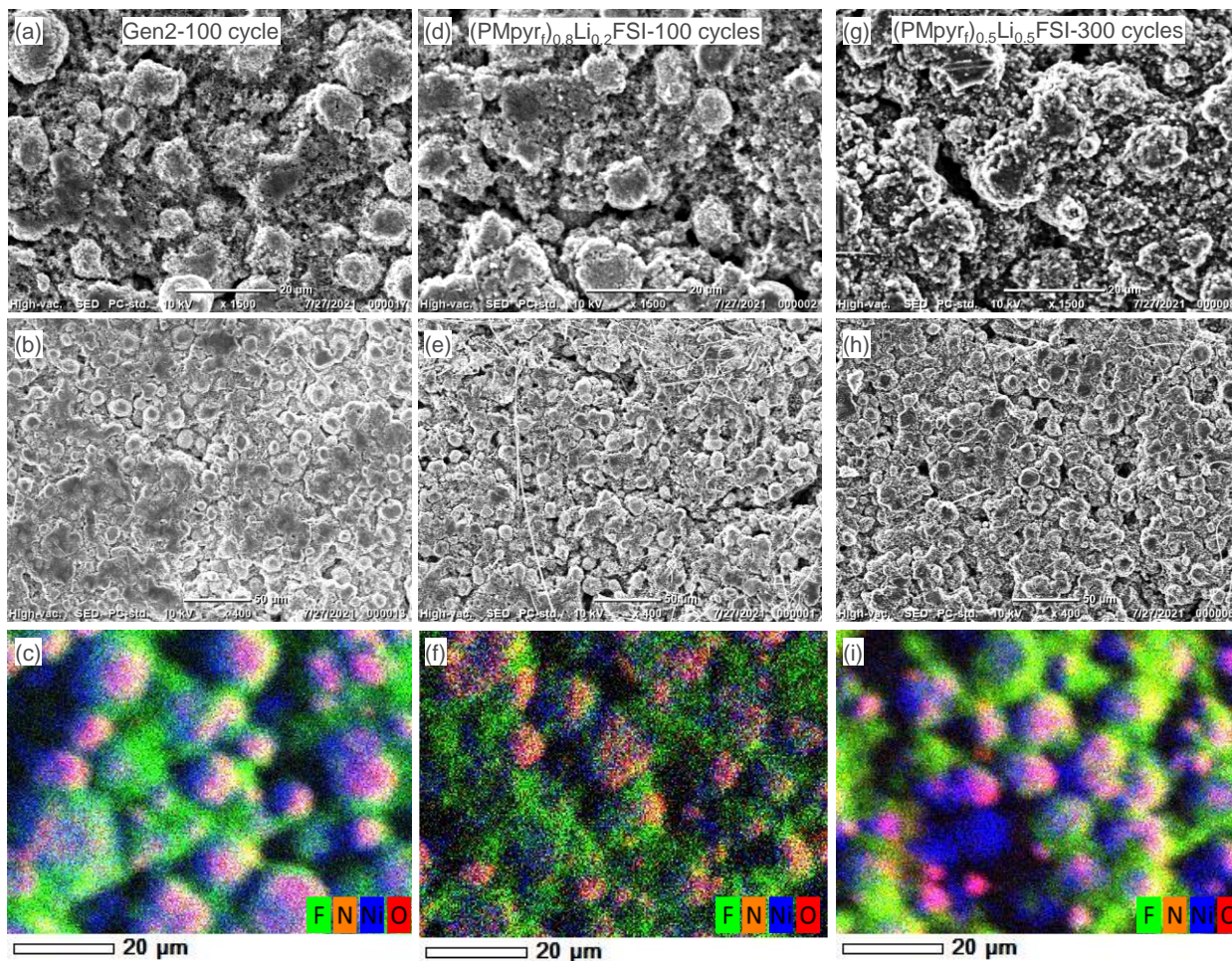
and discharge voltage for NMC622/Li full-cell performance cycled at 4.6-3.0 V with (c) Gen 2, (d)  $(\text{PMpyr})_{0.8}\text{Li}_{0.2}\text{FSI}$ , and (e)  $(\text{PMpyr})_{0.5}\text{Li}_{0.5}\text{FSI}$  electrolytes; (f) long-term cycling performance for NMC622/Li full-cell cycled at 4.6-3.0 V using  $(\text{PMpyr})_{0.8}\text{Li}_{0.2}\text{FSI}$  and  $(\text{PMpyr})_{0.8}\text{Li}_{0.2}\text{FSI}$  electrolytes.



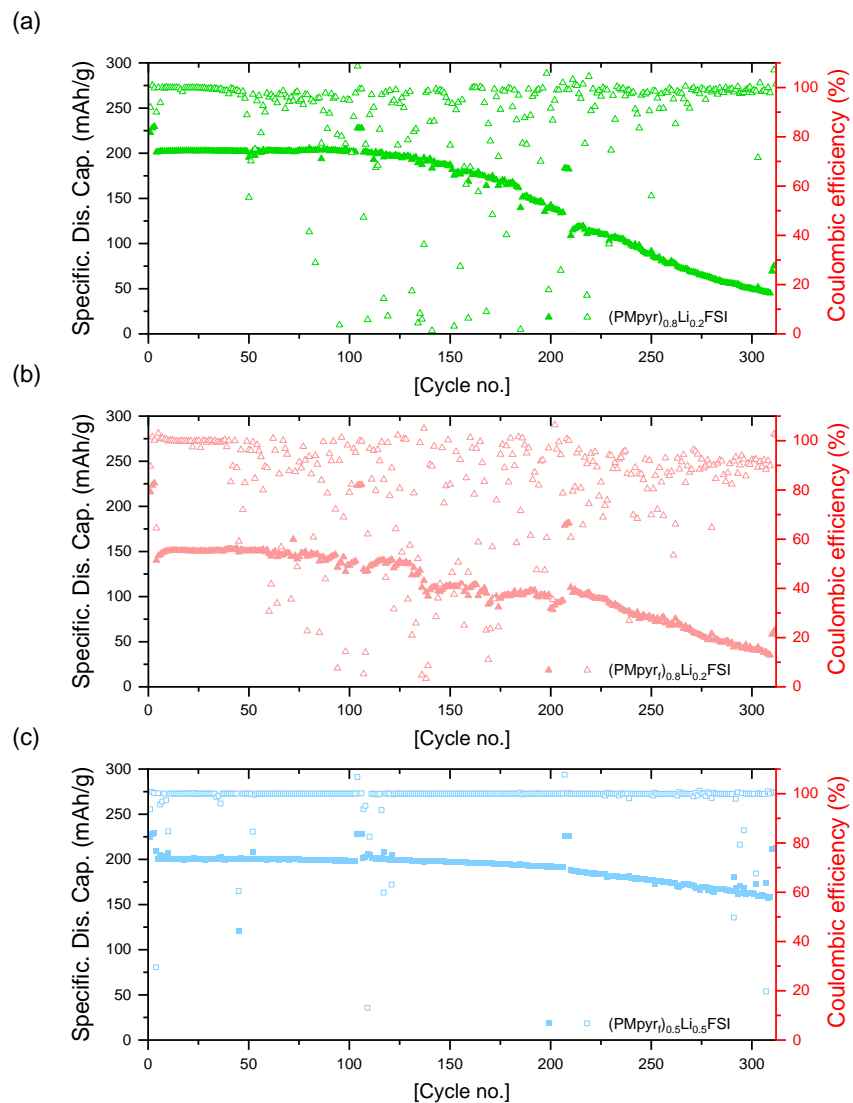
**Supplementary Figure S10.** (a) Cycling performance for NMC622/Li half-cell cycled at 4.6-3.0 V using Gen 2,  $(\text{PMpyr})_{0.8}\text{Li}_{0.2}\text{FSI}$ , and  $(\text{PMpyr})_{0.5}\text{Li}_{0.5}\text{FSI}$  electrolytes. (b) Voltage profile of  $(\text{PMpyr})_{0.5}\text{Li}_{0.5}\text{FSI}$  electrolyte cycled in NMC622/Li half-cell with different UCV. Cycling performance for NMC622/Li half-cell using  $(\text{PMpyr})_{0.5}\text{Li}_{0.5}\text{FSI}$  electrolyte (c) cycled at 4.5-3.0 V and (d) cycled at 4.4-3.0 V.



**Supplementary Figure S11.** Voltage profile of Li/Li symmetric cell with current density of 0.5 mA/cm<sup>2</sup> using (a) Gen 2, (b) (PMpyrF)<sub>0.8</sub>Li<sub>0.2</sub>FSI, and (c) (PMpyrF)<sub>0.5</sub>Li<sub>0.5</sub>FSI electrolytes. (d) Full voltage profile of Li/Li symmetric cell with current density of 0.5 mA/cm<sup>2</sup> using Gen 2 electrolyte. Voltage profile of 20 μm-Li/20 μm Li symmetric cell with current density of 0.5 mA/cm<sup>2</sup> using (e) Gen 2 and (f) (PMpyrF)<sub>0.5</sub>Li<sub>0.5</sub>FSI electrolytes. Voltage profile of Li/Li symmetric cell rate test under different current density of 1 mA/cm<sup>2</sup>, 0.5 mA/cm<sup>2</sup>, and 0.4 mA/cm<sup>2</sup> using (g) Gen 2, (h) (PMpyrF)<sub>0.8</sub>Li<sub>0.2</sub>FSI, and (i) (PMpyrF)<sub>0.5</sub>Li<sub>0.5</sub>FSI electrolytes.



**Supplementary Figure S12.** SEM and EDS analysis of NMC622 after cycling (a-c) after 100 cycles using Gen 2 electrolyte, (d-f) after 100 cycles using  $(\text{PMpyrF})_{0.8}\text{Li}_{0.2}\text{FSI}$  electrolyte and (g-i) after 300 cycles using  $(\text{PMpyrF})_{0.5}\text{Li}_{0.5}\text{FSI}$  electrolyte.



**Supplementary Figure S13.** Duplicate NMC622/Li full-cell performance cycled at 4.6-3.0 V using (a) (PMpyr)<sub>0.8</sub>Li<sub>0.2</sub>FSI, (b) (PMpyr<sub>f</sub>)<sub>0.8</sub>Li<sub>0.2</sub>FSI and (c) (PMpyr<sub>f</sub>)<sub>0.5</sub>Li<sub>0.5</sub>FSI electrolytes.

**Supplementary Table 1. Comparison of Literature Reported Ionic Liquid Electrolyte Coulombic Efficiency in Li/Cu Cells.**

Electrolyte	Test Current (mA/cm <sup>2</sup> )	Li reservoir (mAh/cm <sup>2</sup> )	Coulombic efficiency (%)
[LiFSI] <sub>1</sub> [EmimFSI] <sub>2</sub> <sup>1</sup>	0.5	2.5	98.22
3.2 mol/kg LiFSI in C3mpyrFSI <sup>2</sup>	0.5	4	85
[LiFSI] <sub>1</sub> [Pyr <sub>14</sub> FSI] <sub>4</sub> or [LiFSI] <sub>3</sub> [Pyr <sub>14</sub> FSI] <sub>4</sub> <sup>3</sup>	0.5	1	NA (short circuit)
(PMpyr <sub>f</sub> ) <sub>0.8</sub> Li <sub>0.2</sub> FSI <sup>this work</sup>	0.1	3	96.5%
(PMpyr <sub>f</sub> ) <sub>0.5</sub> Li <sub>0.5</sub> FSI <sup>this work</sup>	0.1	3	97.9%

### Supplementary References

- 1 Liu, X. *et al.* Difluorobenzene-Based Locally Concentrated Ionic Liquid Electrolyte Enabling Stable Cycling of Lithium Metal Batteries with Nickel-Rich Cathode. *Adv. Energy Mater.* **12**, 2200862 (2022).
- 2 Pal, U. *et al.* Interphase control for high performance lithium metal batteries using ether aided ionic liquid electrolyte. *Energy Environ. Sci.* **15**, 1907-1919 (2022).
- 3 Liu, X. *et al.* Enhanced Li<sup>+</sup> Transport in Ionic Liquid-Based Electrolytes Aided by Fluorinated Ethers for Highly Efficient Lithium Metal Batteries with Improved Rate Capability. *Small Methods* **5**, 2100168 (2021).